Optogenetic analysis of synaptic function

Jana F Liewald[1,5], Martin Brauner[1,5], Greg J Stephens[2], Magali Bouhours[3], Christian Schultheis[1], Mei Zhen[3] & Alexander Gottschalk[1,4]

We introduce optogenetic investigation of neurotransmission (OptIoN) for time-resolved and quantitative assessment of synaptic function via behavioral and electrophysiological analyses. We photo-triggered release of acetylcholine or γ-aminobutyric acid at *Caenorhabditis elegans* neuromuscular junctions using targeted expression of *Chlamydomonas reinhardtii* Channelrhodopsin-2. In intact Channelrhodopsin-2 transgenic worms, photostimulation instantly induced body elongation (for γ-aminobutyric acid) or contraction (for acetylcholine), which we analyzed acutely, or during sustained activation with automated image analysis, to assess synaptic efficacy. In dissected worms, photostimulation evoked neurotransmitter-specific postsynaptic currents that could be triggered repeatedly and at various frequencies. Light-evoked behaviors and postsynaptic currents were significantly ($P \leq 0.05$) altered in mutants with pre- or postsynaptic defects, although the behavioral phenotypes did not unambiguously report on synaptic function in all cases tested. OptIoN facilitates the analysis of neurotransmission with high temporal precision, in a neurotransmitter-selective manner, possibly allowing future investigation of synaptic plasticity in *C. elegans*.

Much of our understanding of the mechanisms of chemical synaptic transmission comes from the analysis of mutants that are compromised in pre- or postsynaptic functions. Such mutants could be affected in synaptic-vesicle biogenesis, neurotransmitter loading, active zone translocation, vesicle priming, fusion and recycling[1,2] or biogenesis, surface expression and function of neurotransmitter receptors[3]. Lesions in synaptic transmission are analyzed at the single-synapse level by electrophysiology or imaging[4] and at the behavioral level using pharmacological synaptic perturbation[5].

The neuromuscular junction of the nematode *C. elegans* is a key genetic model for examining molecular mechanisms of neurotransmission[6,7]. The basic protein machineries involved in mammalian neurotransmission are conserved in *C. elegans*[1,2,5,8]. Most *C. elegans* mutants with severe neurotransmission defects are viable, and adult worms can thus be analyzed. However, many state-of-the-art physiological tools are technically challenging to implement in the worm. For electrophysiological analysis at neuromuscular junctions, worms must be dissected to access the muscle cells for patch-clamp analysis, and motoneurons are stimulated by electric or osmotic shock, which activates the readily releasable pool of synaptic vesicles[6,7]. This is challenging because of the small size of the preparation. Also, the current protocol is limited in its utility. First, the approach cannot be used to distinguish between cholinergic and γ-aminobutyric acid (GABA)-ergic inputs. Second, electric shocks are variable and cause tissue damage, thus only low-frequency electrical stimulation has been reported[9]. Furthermore, methods allowing physiological *in vivo* synaptic stimulation, which could facilitate analysis of synaptic efficacy and plasticity in intact worms, are not established. To this end, we previously developed optogenetic methods, using the light-gated cation channel Channelrhodopsin-2 (ChR2), for precise photoinduced depolarization of muscle cells or neurons in live and dissected transgenic *C. elegans*[10–12]. Similar approaches have been reported for vertebrate systems[13–15].

Here we introduce optogenetic investigation of neurotransmission (OptIoN), which allows selective, reproducible and repetitive high-frequency photostimulation of cholinergic or GABAergic neurons. By analyzing in a quantitative and time-resolved manner the photoinduced electrical activity in dissected neuromuscular junctions as well as photo-evoked behavioral changes in the intact worm, we can examine *C. elegans* mutants for defects in various aspects of synaptic function.

RESULTS

Sensitizing cholinergic and GABAergic motoneurons to light

At the *C. elegans* neuromuscular junction, body-wall muscle cells are innervated by both cholinergic (excitatory) and GABAergic (inhibitory) motoneurons[16] (**Supplementary Fig. 1a** online). To selectively sensitize these neurons to light-induced depolarization, we created artificial transgenes to selectively express ChR2 (amino acids 1–315) fused to YFP (GenBank accession AF461397; we also introduced the H134R mutation, as previously described[11]) in these cells, using two cell type–specific promoters: (i) we used P*unc-47*, which normally drives expression of the vesicular GABA transporter vGAT[17], to express ChR2-YFP in GABAergic neurons (from the

[1]Institute of Biochemistry, Department of Biochemistry, Chemistry and Pharmacy, Goethe University Frankfurt, Biocenter N220, Max von Laue Str. 9, D-60438 Frankfurt, Germany. [2]Lewis Sigler Institute for Integrative Genomics, Carl Icahn Laboratory, Washington Road, Princeton University, Princeton, New Jersey 08544, USA. [3]Samuel Lunenfeld Research Institute, Mount Sinai Hospital, 600 University Ave., Toronto, Ontario M5G 1X5, Canada. [4]Cluster of Excellence Frankfurt—Macromolecular Complexes, Goethe University, Max von Laue Str. 3, D-60438 Frankfurt, Germany. [5]These authors contributed equally to this work. Correspondence should be addressed to A.G. (a.gottschalk@em.uni-frankfurt.de).

RECEIVED 28 MARCH; ACCEPTED 22 AUGUST; PUBLISHED ONLINE 14 SEPTEMBER 2008; DOI:10.1038/NMETH.1252

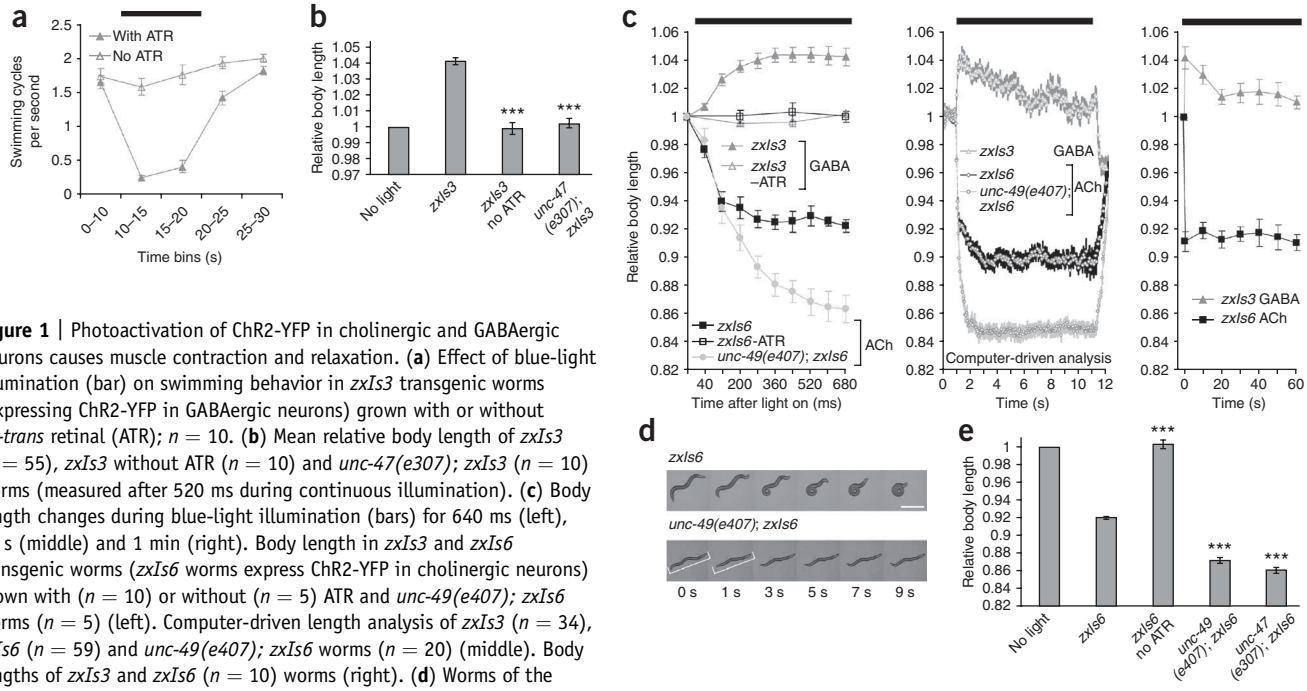

Figure 1 | Photoactivation of ChR2-YFP in cholinergic and GABAergic neurons causes muscle contraction and relaxation. (**a**) Effect of blue-light illumination (bar) on swimming behavior in *zxIs3* transgenic worms (expressing ChR2-YFP in GABAergic neurons) grown with or without all-*trans* retinal (ATR); $n = 10$. (**b**) Mean relative body length of *zxIs3* ($n = 55$), *zxIs3* without ATR ($n = 10$) and *unc-47(e307)*; *zxIs3* ($n = 10$) worms (measured after 520 ms during continuous illumination). (**c**) Body length changes during blue-light illumination (bars) for 640 ms (left), 10 s (middle) and 1 min (right). Body length in *zxIs3* and *zxIs6* transgenic worms (*zxIs6* worms express ChR2-YFP in cholinergic neurons) grown with ($n = 10$) or without ($n = 5$) ATR and *unc-49(e407); zxIs6* worms ($n = 5$) (left). Computer-driven length analysis of *zxIs3* ($n = 34$), *zxIs6* ($n = 59$) and *unc-49(e407); zxIs6* worms ($n = 20$) (middle). Body lengths of *zxIs3* and *zxIs6* ($n = 10$) worms (right). (**d**) Worms of the indicated genotype were imaged during 10-s illumination. Scale bar, 0.5 mm. (**e**) Mean relative body length of *zxIs6* ($n = 115$), *zxIs6* without ATR ($n = 5$), *unc-49(e407); zxIs6* ($n = 45$) and *unc-47(e307); zxIs6* ($n = 20$) worms (520-ms illumination). To yield functional ChR2, ATR was added to growth media, unless otherwise stated. ***$P < 0.001$; error bars, s.e.m.

integrated transgene *zxIs3*); and (ii) we used P*unc-17*, which normally drives expression of the vesicular acetylcholine (ACh) transporter vAChT[18], to express ChR2-YFP in cholinergic neurons (from the integrated transgene *zxIs6*). YFP fluorescence was evident at the plasma membrane of neuronal somata, and along dorsal and ventral nerve cord processes; we verified normal structure of the nervous system in the strains used (**Supplementary Fig. 2** online). To provide the chromophore, essential for ChR2 function, we grew transgenic worms on medium containing all-*trans* retinal.

Light-induced GABA or ACh release alters body length

When we activated ChR2-YFP in *zxIs3* (GABA) worms swimming in liquid by applying 450–490 nm light, normal swimming behavior became almost completely blocked (**Fig. 1a** and **Supplementary Video 1** online). On a solid substrate, illuminated *zxIs3* worms exhibited almost complete paralysis, presumably because of simultaneous relaxation of all body-wall muscle cells (**Supplementary Video 2** online). The body also elongated up to 104.1 ± 0.2% of the initial length, within ~350 ms (**Fig. 1b,c**; values were measured after 520 ms using graphics software). We could trigger this behavior repeatedly, and it fully reversed in the dark (**Fig. 1c** and data not shown). During 10 s of illumination, worms partially recovered from paralysis after ~3 s, that is, elongation slowly decreased (**Fig. 1c**), and they resumed moving, though in an uncoordinated fashion and with reduced speed (**Supplementary Video 2** and data not shown). However, worms remained partially elongated even after 60 s, suggesting sustained GABA release (**Fig. 1c**; 101.1 ± 0.4%). Elongation was abolished in *unc-47(e307)* mutants that lacked the vGAT (**Fig. 1b** and **Supplementary Video 3** online), indicating that elongation depended on GABA-filled synaptic vesicles. Neither transgenic worms grown without all-*trans* retinal (**Fig. 1a–c**), nor wild-type worms grown with or without all-*trans* retinal showed any of these effects when illuminated[11,12].

When we photostimulated cholinergic neurons in worms expressing the transgene *zxIs6*, either for 10 s or 60 s (**Fig. 1c,d**) or 10 ms (**Supplementary Fig. 1b**), worms showed rapid body contraction to 92.0 ± 0.2% of the initial body length (**Fig. 1c,e** and **Supplementary Videos 4** and **5** online). Contractions reached a maximal level after 200–300 ms; however, unless we reported time courses, the reported values were obtained after 520 ms of illumination (**Supplementary Table 1** online). Contractions were sustained during 60 s of illumination (**Fig. 1c**). Additionally, within ~10 s of illumination, dorsal coiling of the worms was triggered ($n = 20$; **Fig. 1d** and **Supplementary Video 4**). Concomitant GABA release, indirectly triggered by photoactivation of cholinergic neurons innervating GABAergic neurons[16,19] (**Supplementary Fig. 1a**), may cause the coiling and reduce the extent of evoked contractions. Indeed, *unc-49(e407)* worms[20], lacking the ionotropic $GABA_A$ receptor ($GABA_AR$) in muscle, and *unc-47(e307)* vGAT mutants showed no coiling (**Supplementary Video 6** online) and stronger shortening (to 86–87% of the initial length; **Fig. 1c–e**).

As the promoter P*unc-17* is known to be active in a few interneurons as well as in the cholinergic motoneurons, we examined transgenic worms expressing ChR2-YFP from another cholinergic, motoneuron-specific but weaker promoter, P*unc-4*. Again we observed contraction and coiling upon illumination but to a milder degree. Thus, shrinking and coiling appear to be due to ChR2 activity in cholinergic motoneurons, and the extent of the effect depends on the amount of ChR2-YFP expressed (**Supplementary Fig. 1c**). Transgenic *zxIs6* worms grown without all-*trans* retinal neither contracted (**Fig. 1c,e**) nor coiled during illumination.

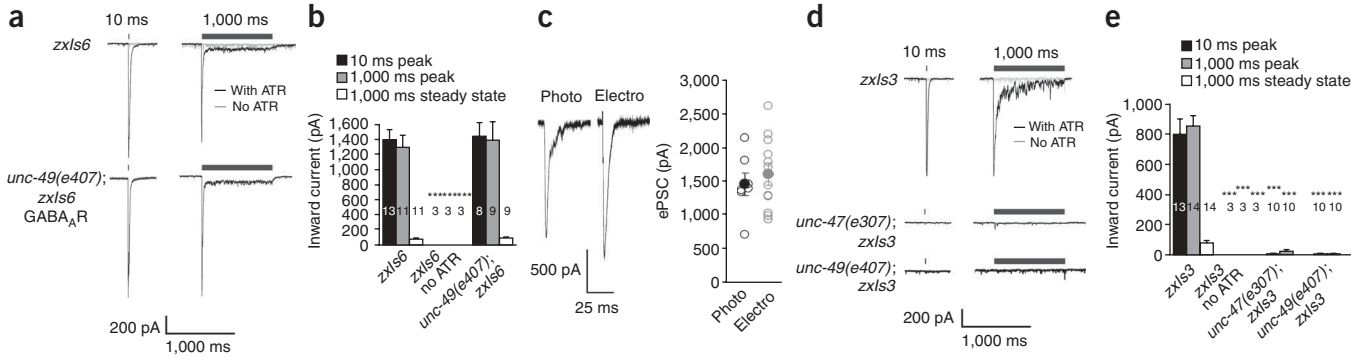

Figure 2 | Light-induced ACh or GABA release evokes postsynaptic currents at the neuromuscular junction. (**a**–**e**) Representative traces for ACh-mediated (**a**) and GABA-mediated (**d**) inward currents evoked by photostimuli (bars) of 10 or 1,000 ms in the presence and absence of all-*trans* retinal (ATR). Mean peak values of currents evoked in the presence of ATR by 10-ms and 1,000-ms illumination (ACh (**b**) and GABA (**e**); *n* values indicated in the bars). GABA photo-ePSCs are outward because of the high Cl^- concentration in the patch pipette. Representative traces of PSCs (**c**) evoked by a 10-ms photostimulus or electrostimulus. Mean values of ePSCs did not differ for photo- ($n = 7$) and electrical ePSCs ($n = 12$). ATR was added to growth media, unless otherwise stated.

Quantitative analysis of prolonged light-evoked behaviors

Analyzing the time course of both acute and long-lasting light-evoked behaviors at high temporal resolution could provide information about synaptic performance. Using software we had developed[21], we collected automated measurements of worm body length in individual movie frames before, during and after illumination. As we observed by manual quantification, *zxIs6* worms contracted to about 90% of the original length and remained contracted during the 10-s stimulus, whereas *unc-49(e407);zxIs6* mutants sustained contractions to ~85% (**Fig. 1c** and **Supplementary Fig. 3** online). In *zxIs3* worms, photostimulation triggered elongation within ~500 ms, which lasted for the entire 10 s of illumination, though the length slowly decreased from an initial 104.5% to ~102% (**Fig. 1c**).

Light-induced ACh or GABA release evokes photo-ePSCs

To measure photo-evoked transmitter release at the cellular level, we performed whole-cell voltage-clamp recordings from body-wall muscle cells. The frequency and amplitude of endogenous miniature postsynaptic currents of ChR2-YFP-expressing worms were comparable to those in the wild type (**Supplementary Fig. 4a** online). Postsynaptic physiology was normal in worms expressing ChR2-YFP (**Supplementary Fig. 4b**).

In *zxIs6* and *zxIs3* transgenic worms grown without all-*trans* retinal, photostimulation evoked no postsynaptic currents. However, in *zxIs6* (ACh) worms raised with all-*trans* retinal, 10-ms blue light pulses induced evoked postsynaptic currents (ePSCs) of 1,401 ± 126 pA, which were neurotransmitter-specific, fast and peaked after ~5 ms (**Fig. 2a**,**b**). These light-induced ePSCs (from now on termed photo-ePSCs) were mediated by ACh only, with no contribution from ACh-induced GABA release, as we observed equivalent photo-ePSCs in *unc-49(e407)* $GABA_AR$ mutants (**Fig. 2a**,**b**) and the evoked currents could be blocked by tubocurare (**Supplementary Fig. 4c**). Photo-evoked ACh ePSCs generally compared well to electrically evoked ePSCs, displaying similar kinetics, and could be manipulated to comparable amplitudes by modulating the intensity of the stimuli (**Fig. 2c**).

Electric stimulation does not generate GABA ePSCs, for unknown reasons[22]. Notably, using OptIoN, we recorded GABA ePSCs after GABA motoneuron–specific photoactivation: 10-ms photostimuli on *zxIs3* worms induced photo-ePSCs of 803 ± 102 pA (**Fig. 2d**,**e**). These photo-ePSCs were GABA-evoked because they were abolished in *unc-47(e307)* vGAT mutants and in *unc-49(e407)* $GABA_AR$ mutants (**Fig. 2d**,**e**). In addition, they were not affected by the presence of tubocurare (**Supplementary Fig. 4c**).

Finally, in contrast to electric stimulation, OptIoN allows prolonged, continuous stimulation. In both *zxIs6* and *zxIs3* strains, 1-s photostimulation induced peak ePSCs (ACh, 1,299 ± 157 pA; GABA, 855 ± 65 pA; **Fig. 2a**,**b**,**d**,**e**). Currents decreased to small steady-state levels persisting as long as the illumination (ACh, 79 ± 8 pA (6% of peak); GABA, 80 ± 17 pA (9% of peak)). How these ePSCs correlate with the activity of motoneurons in intact worms during prolonged illumination and, notably, during normal physiological neurotransmission in the worm, is unknown.

Analyzing defective GABA neurotransmission by OptIoN

Using photo-induced GABA release, we investigated whether GABAergic synaptic defects in various mutants correlated at the behavioral and cellular levels. In *unc-47(e307)* vGAT mutants, which did not show GABA photo-ePSCs (**Fig. 2d**,**e**), we also could not photo-evoke relaxation (**Fig. 1b**, **Supplementary Video 3** and **Supplementary Table 1**). We made analogous observations in *unc-64(js115)* mutants, which lack the t-SNARE syntaxin specifically in GABAergic neurons[23]. Consistent with syntaxin's role in synaptic-vesicle exocytosis[24], GABA photo-ePSCs were drastically reduced (**Fig. 3a**,**b**), and photo-evoked relaxation was severely impaired (**Fig. 3c** and **Supplementary Table 2** online).

Our assay appears to be also sufficiently sensitive to reveal defects in weak neurotransmission mutants. *snb-1(md247)* mutants, which harbor a mild reduction-of-function mutation in the v-SNARE synaptobrevin[25], showed reduced body elongation immediately after photostimulation (**Fig. 3c**); however, they displayed a wild-type phenotype after ~1 s of photostimulation (**Supplementary Fig. 3b**). One interpretation of this result is that GABA release in *snb-1(md247)* mutants is initially insufficient to evoke a response, but that sufficient GABA may accumulate at the synaptic cleft during sustained stimulation.

We also analyzed mutants in synaptotagmin, the Ca^{2+} sensor for fast synchronous release of primed synaptic vesicles, which additionally acts in synaptic-vesicle endocytosis[26,27]. *snt-1(md290)*

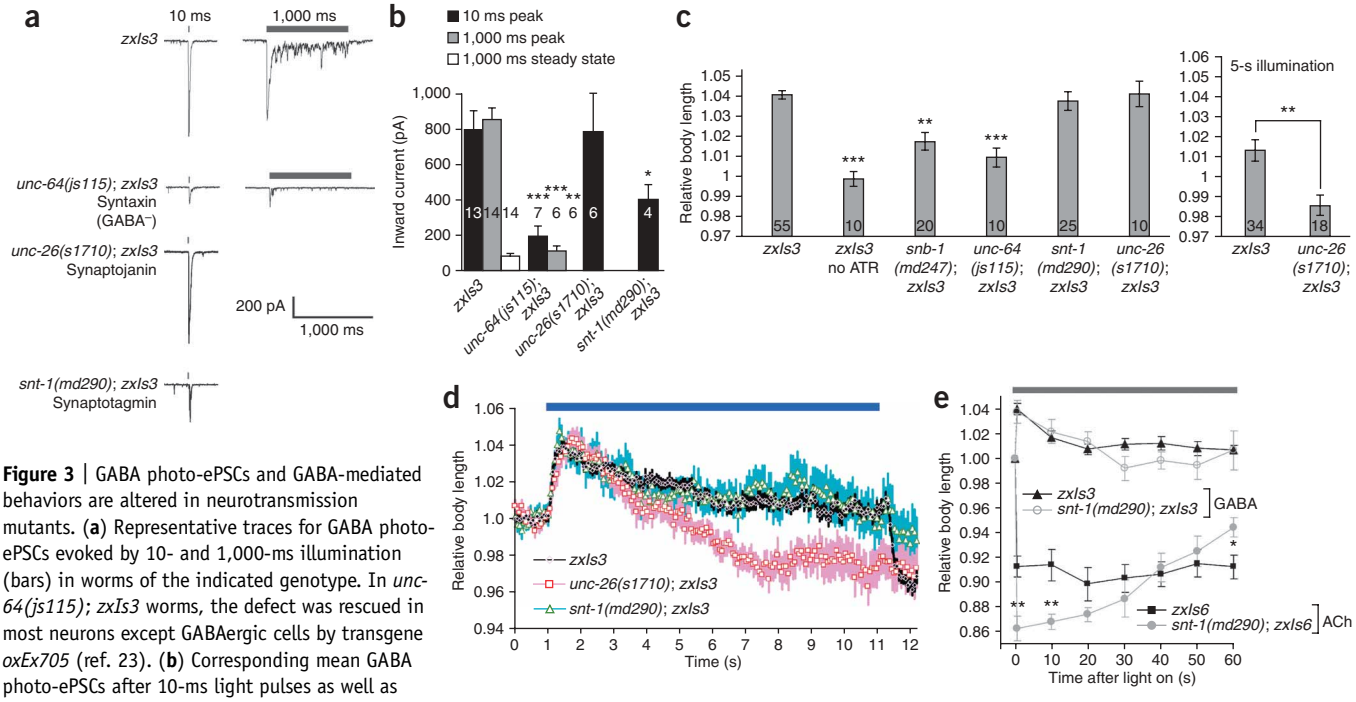

Figure 3 | GABA photo-ePSCs and GABA-mediated behaviors are altered in neurotransmission mutants. (**a**) Representative traces for GABA photo-ePSCs evoked by 10- and 1,000-ms illumination (bars) in worms of the indicated genotype. In *unc-64(js115); zxIs3* worms, the defect was rescued in most neurons except GABAergic cells by transgene *oxEx705* (ref. 23). (**b**) Corresponding mean GABA photo-ePSCs after 10-ms light pulses as well as peak and steady-state currents after 1,000-ms light pulses. (**c**) Mean relative body length after 520 ms (left) or 5 s (right) of light-induced GABA release in worms of indicated genotypes in the presence of all-*trans* retinal (ATR). *zxIs3* worms grown without ATR were analyzed as a control. (**d**) Relative body length after long-term photostimulation (bar) assayed by computer-driven analysis of worm shape. *zxIs3* ($n = 39$) and mutants with impaired neurotransmission, *snt-1(md290); zxIs3* ($n = 13$) and *unc-26(s1710); zxIs3* ($n = 18$), were compared during light-induced GABA release. (**e**) Long-term photostimulation of transgenic worms of the indicated genotype for 60 s ($n \geqslant 10$ for all genotypes). Statistically significant differences in all graphs refer to transgene-only values. ATR was added to growth media, unless otherwise stated. $^*P < 0.05$, $^{**}P < 0.01$ and $^{***}P < 0.001$; error bars, s.e.m. Numbers in **b** and **c** are *n* values for each experiment.

null mutants are severely uncoordinated, and GABA-ePSCs were largely reduced in these worms (**Fig. 3a,b** and **Supplementary Table 2**). Notably, GABA-mediated body elongation did not differ from the wild type, either after short or long-term photostimulation (**Fig. 3c–e**). The reason for this discrepancy between photo-evoked behavior and ePSCs is currently unclear; possibly asynchronous GABA release masked defects during prolonged stimulation.

Analyzing defective ACh neurotransmission by OptIoN

Using photoinduced ACh release, we investigated whether cholinergic synaptic defects in various mutants correlated at the behavioral and cellular levels. In worms with mutations in synaptotagmin, *snt-1(md290)*, the synaptic vesicle priming factor *unc-13*(*n2813* and *e1091)* (ref. 28, partial and strong loss-of-function alleles, respectively), and the phospholipid phosphatase synaptojanin, *unc-26(s1710)* (ref. 29), which is Tgene, required for endocytic recycling of synaptic vesicles, we found drastically reduced ACh photo-ePSCs (**Fig. 4a,b** and **Supplementary Table 2**), consistent with previously reported electrically evoked PSCs in some of these mutants[9,28].

Unexpectedly, the behavioral responses of these mutants did not follow the anticipated pattern. Although OptIoN reported altered behavior for presynaptic mutants upon photo-induced ACh release, the photo-evoked contractions were significantly stronger ($P \leq 0.05$; **Supplementary Table 1**) when compared to those in wild-type worms, thus contradictory to the decreased ACh photo-ePSCs observed. For instance, light-evoked contractions in *snt-1(md290)* mutants (**Figs. 3e** and **4c,d** and **Supplementary Table 1**) resulted in relative body lengths of 87.5 ± 1.3% ($n = 10$); compared to 92.0 ± 0.2% for wild type ($P = 0.0018$). We observed increased contractions in all presynaptic mutants tested (**Fig. 4c**), including *snb-1(md247)*, *unc-13(n2813)*, *unc-13(e1091)*, *unc-26(s1710)* (ref. 29) and in a mutant in an AP180 clathrin adaptor homolog involved in endocytosis, *unc-11(e47)* (ref. 30). These paradoxical results are at least partially due to compensatory mechanisms in muscle (**Supplementary Fig. 5** and **Supplementary Results** online). These results emphasize that to characterize a particular synaptic mutation, behavioral assays must be complemented with additional experiments.

Repeated photostimulation at various frequencies

We next tested whether ChR2-YFP could enable repeated, possibly even high-frequency stimulation, which is critical for studying defects in synaptic-vesicle recycling and synaptic plasticity. Repetitive, 10-ms light pulses at frequencies between 0.5 and 50 Hz evoked robust and reliable ACh and GABA photo-ePSCs (**Fig. 5a,b** and **Supplementary Fig. 6** online). The amplitude of subsequent currents decreased to 70–85% of that evoked by the initial stimulus for both ACh and GABA neurons at 0.5 Hz or to 52–57% (GABA) and 48–47% (ACh) at 2 Hz. At 35 Hz, some of the later stimuli did not evoke currents. Photo-ePSCs in response to 50-Hz stimuli resembled permanently illuminated samples, that is, exhibiting 'steady-state' currents (data not shown).

The reduction in the magnitude of consecutive ePSCs could represent presynaptic depression or rundown, or desensitization of postsynaptic receptors. To investigate whether ChR2 desensitization also contributes to the rundown, we applied either single

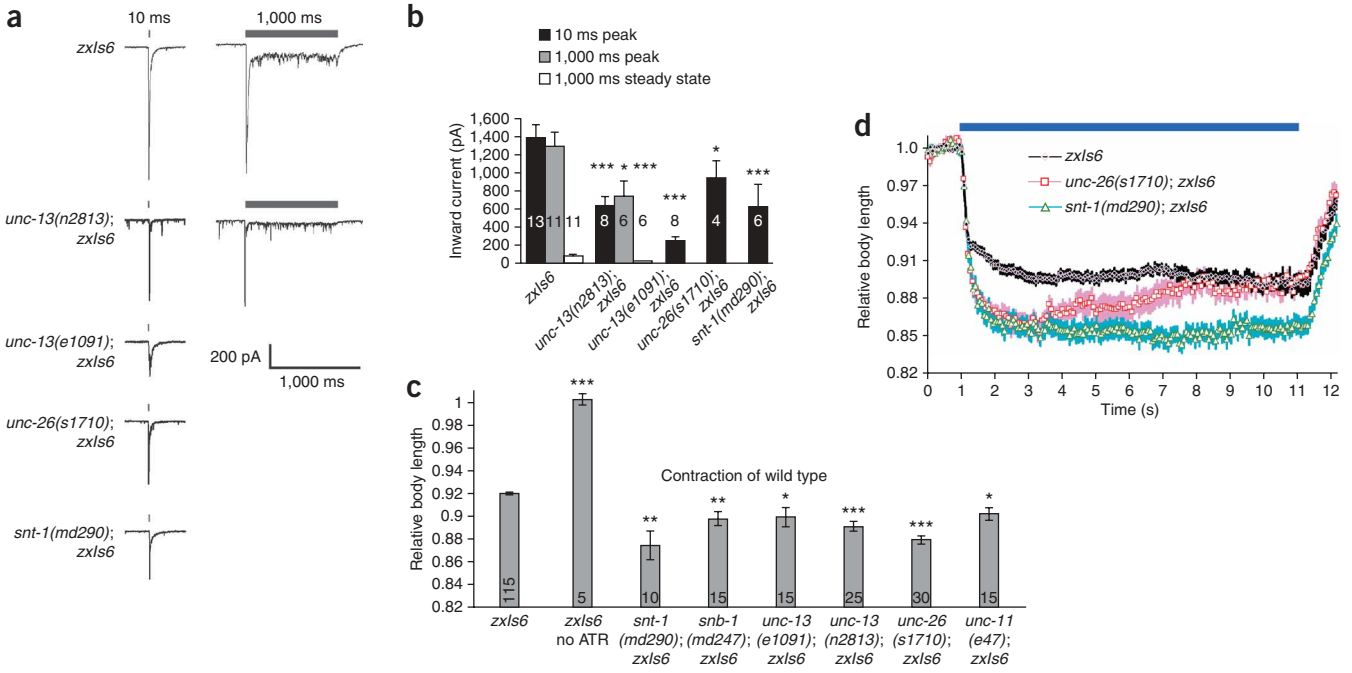

Figure 4 | ACh photo-ePSCs and ACh-mediated behaviors are altered in neurotransmission mutants. (**a**) Representative traces for ACh photo-ePSCs evoked by 10- and 1,000-ms illumination (bars) in worms of the indicated genotype. (**b**) Corresponding mean ACh photo-ePSCs. (**c**) Mean relative body length after 520 ms of light-induced ACh release in worms of the indicated genotypes in the presence of all-*trans* retinal (ATR). As a control, wild-type worms grown in the absence of ATR were also analyzed. Numbers in **b** and **c** are *n* values for each experiment. (**d**) Relative body length after long-term photostimulation (bar) assayed by computer-driven analysis of worm shape. Wild type ($n = 59$) and mutants with impaired neurotransmission, *snt-1(md290)*; *zxIs6* ($n = 27$) and *unc-26(s1710)*; *zxIs6* ($n = 16$) were compared during light-induced ACh release. ATR was added to growth media, unless otherwise stated. $*P < 0.05$, $**P < 0.01$ and $***P < 0.001$; error bars, s.e.m.

stimuli or 2-Hz stimulus trains including 20-s or 60-s dark periods (interstimulus or intertrain intervals). We observed that ePSCs after 20-s interstimulus intervals or the first ePSCs in trains with 20-s intertrain intervals recovered to initial values (**Supplementary Figs. 7** and **8** online); thus ChR2 requires 10–20 s for full recovery, as reported in other systems[10,11,13]. Hence, although ChR2 desensitization may contribute to the steep drop from first to second ePSC at higher frequencies, it should not affect rundown in consecutive ePSCs at lower frequencies (0.5 Hz; **Fig. 5a**,**b** and **Supplementary Fig. 6**).

At intermediate frequencies, photostimulation evoked trains of ePSCs decayed with similar kinetics as those evoked by electrical stimulation but with higher reproducibility (2 Hz, **Fig. 5c**,**d**; 0.5 Hz, **Supplementary Fig. 6e**,**f**; compare also to published results[9]). Electrical stimulation

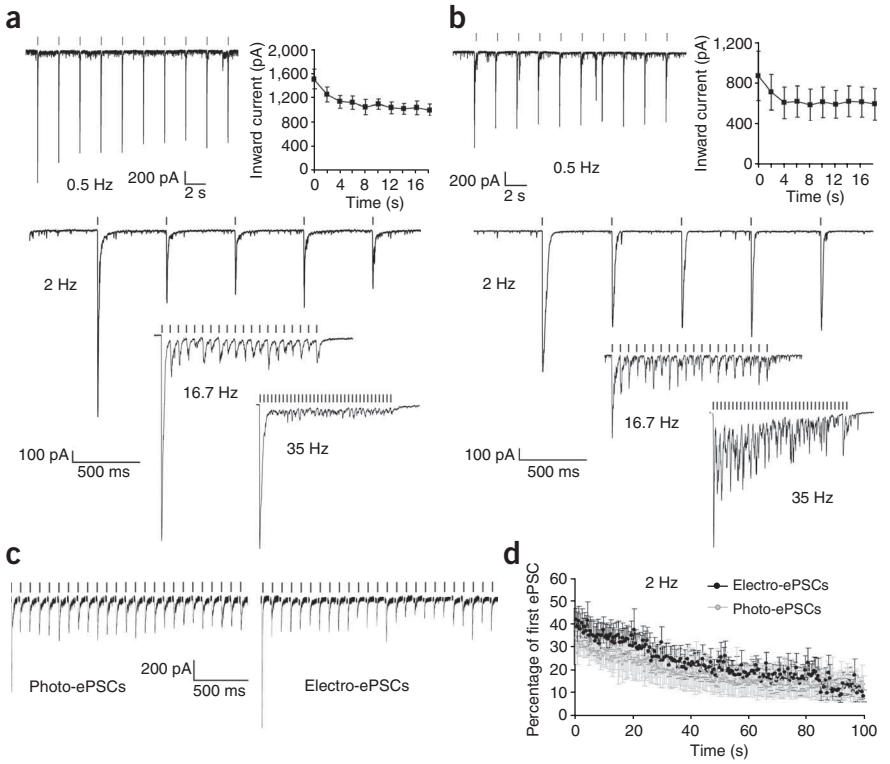

Figure 5 | ACh and GABA photo-ePSCs and ACh-electro-ePSCs during repeated stimulation. (**a**,**b**) Currents evoked by repeated photostimulation (10-ms pulses) at various frequencies (0.5, 2, 16.7 and 35 Hz) and representative traces for ACh (**a**) and GABA (**b**) photo-ePSCs. Mean inward currents at 0.5 Hz ($n = 5$ each) (top right). Worms were wild type, apart from *zxIs6* (ACh) or *zxIs3* (GABA) transgene. (**c**) Representative traces of ePSCs evoked by repeated stimulation at 2 Hz. (**d**) Mean values of currents normalized relative to the first ePSC were not different for photo-evoked ($n = 6$) and electro-evoked ($n = 11$) ePSCs. ATR was added to growth media, unless otherwise stated. Error bars, s.e.m.

did not evoke more than a handful of ePSCs at 20 Hz (data not shown). Thus, photostimulation is a technically far less demanding, more versatile and more reproducible way to trigger ePSCs at both low and high frequencies in a neurotransmitter-specific fashion.

Analyzing defects in synaptic-vesicle priming and recycling

The frequency-dependent rundown of consecutive ePSCs, which we observed under conditions that challenge the synapse (that is, with repeated photostimulation), is likely to reflect at least to some extent a depletion of the readily releasable pool of synaptic vesicles (**Fig. 5** and **Supplementary Fig. 6**). We reasoned that alterations in the synaptic-vesicle cycle could be reflected in a change in the rate of rundown and could therefore be studied using long-term photostimulation. To investigate whether OptIoN is useful for electrophysiological analysis of defective synaptic-vesicle priming and recycling, we analyzed mutants with known defects in these processes.

In the absence of UNC-13 function, which primes synaptic vesicles for fusion, the size of the readily releasable pool of synaptic vesicles is reduced, even though the number of docked vesicles is increased[1,24,28]. Photo-ePSCs at 2 Hz in *unc-13(n2813)* and *unc-13 (e1091)* were significantly reduced compared to those in wild-type worms, for all successive stimuli ($P < 0.001$; **Fig. 6a,b**). Normalized ePSCs were also significantly smaller ($P < 0.05$) in *unc-13* mutants for ~20 stimuli (**Fig. 6c** and **Supplementary Fig. 6e**). These results indicate that *unc-13* mutants have decreased synaptic-vesicle fusion, which may be due to impairment in synaptic-vesicle priming for sustained release, but definitively establishing the defective step in the cycle would require further studies. Also, although the wild type

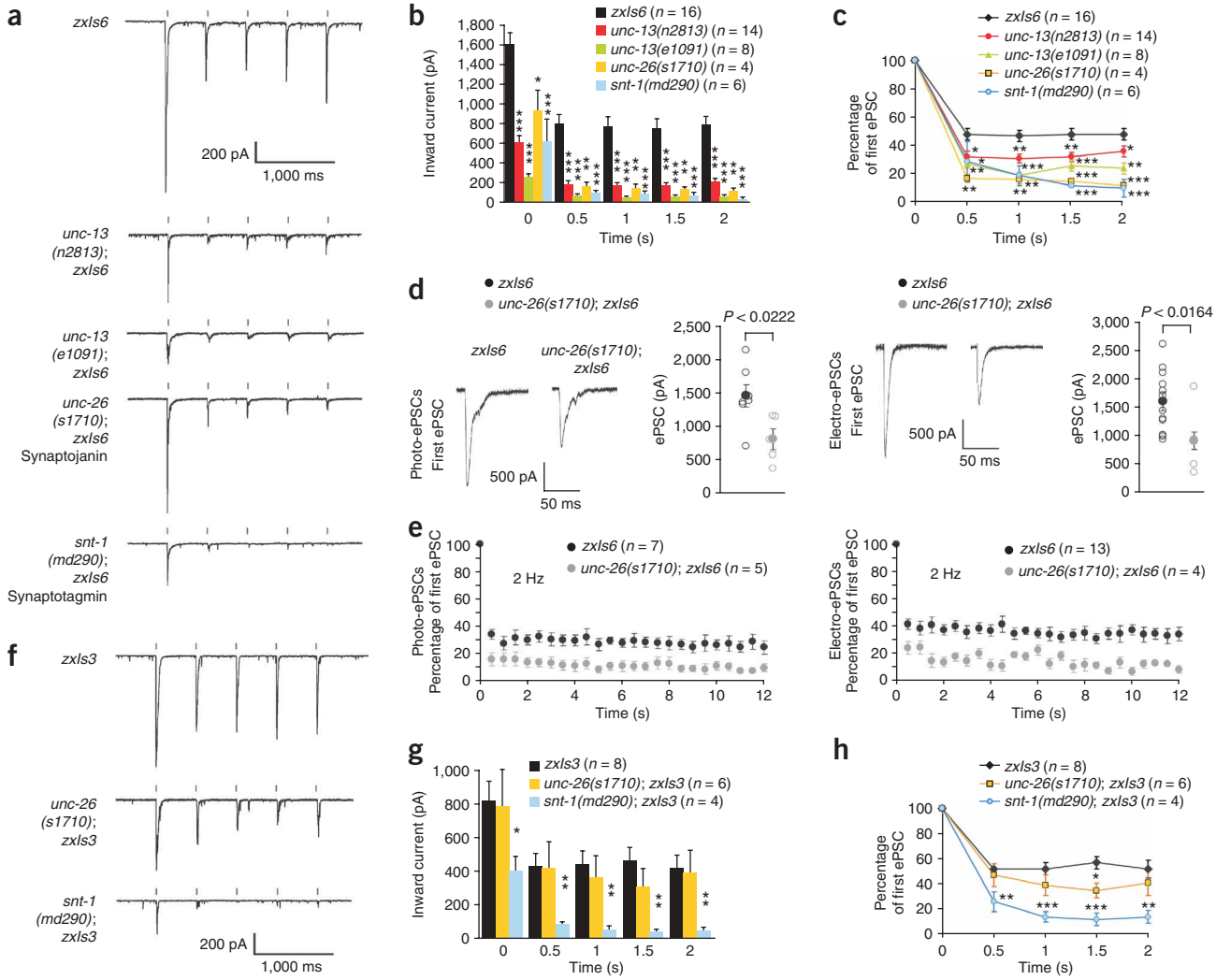

Figure 6 | ACh and GABA photo-ePSCs during repeated photostimulation are altered in neurotransmission mutants implicated in synaptic-vesicle priming and recycling. (**a**) Representative traces for ACh photo-ePSCs evoked by five consecutive 10-ms light pulses at 2 Hz, measured in worms of the indicated genotypes. (**b**,**c**) Mean ACh photo-ePSCs (**b**) and ACh photo-ePSCs normalized relative to the first evoked current (**c**) in the same worms. All worms carry the *zxIs6* transgene. (**d**,**e**) Photo- and electro-evoked ACh PSCs compared in *zxIs6* and *unc-26(s1710); zxIs6* worms. (**d**) Representative traces of PSCs evoked by single 10-ms stimuli (left) and mean values of currents evoked by single 10-ms stimuli (right). (**e**) ACh photo- and electro-evoked ePSCs triggered by 2-Hz stimulus trains. (**f**) Representative traces for GABA photo-ePSCs evoked by five consecutive 10-ms light pulses at 2 Hz, measured in worms of the indicated genotypes. All worms carry the transgene *zxIs3*. (**g**,**h**) Mean GABA photo-ePSCs (**g**) and GABA photo-ePSCs normalized relative to the first evoked current (**h**) in the same worms. ATR was added to growth media. Statistically significant differences in all graphs refer to transgene-only values. $*P < 0.05$, $**P < 0.01$ and $***P < 0.001$; error bars, s.e.m.

showed less depression in synaptic transmission early during the photostimulus train, after ~40 photostimuli, normalized photo-ePSCs in the wild type decreased below those in *unc-13(n2813)* (**Supplementary Fig. 6e**). It is possible that the reserve pool of synaptic vesicles in wild type depletes faster than in the *unc-13* mutant because of more efficient priming in the wild type.

Synaptojanin *unc-26(s1710)* mutants are defective in synaptic-vesicle budding and uncoating during clathrin-mediated endocytosis[9,29]. Consistent with previous studies[9,29], the first ACh photo-ePSC was reduced, and consecutive ePSCs (5 stimuli, 2 Hz) were significantly reduced as compared to wild type ($P < 0.01$; **Fig. 6a–c**). Direct comparison of electro- and photostimulus trains (2 Hz; **Fig. 6d,e**; 0.5 Hz, data not shown) in *unc-26(s1710)* mutants confirmed these findings, further proving the power of the photostimulation system as an accurate but much easier way of assaying synaptic function.

The recycling defect was also reflected in long-term behavioral analysis: When we photostimulated ACh release for 10 s, wild-type worms sustained constant contraction throughout the illumination, while the initially exaggerated body contraction of *unc-26(s1710)* worms returned to wild-type level after 2–3 s (**Fig. 4d**). We observed similar results during prolonged GABA release: initially normal elongation of *unc-26(s1710)* worms dropped below wild-type level within 4 s (**Fig. 3c,d**). Normalized GABA photo-ePSCs in *unc-26* mutants were significantly different to those in wild type only for the fourth stimulus during a 2-Hz, 5-stimulus train ($P < 0.05$; **Fig. 6f–h**). This was possibly due to the brevity of the experiment; behavioral experiments that showed clear differences lasted longer and involved constant stimulation (10 s; **Fig. 3d**).

Lastly, for synaptotagmin, OptIoN revealed effects consistent with its mediation of fast synchronous synaptic-vesicle release, but also its proposed role in synaptic-vesicle recycling[26]. During 2-Hz stimulus trains, *snt-1(md290)* mutants showed severe decay in consecutive normalized photo-ePSCs in response to stimulation of both cholinergic and GABAergic neurons (**Fig. 6a–c,f–h**). The effect on behavior was also consistent with a defect in synaptic-vesicle recycling in cholinergic neurons, as evoked contractions in response to ACh, though initially stronger in *snt-1(md290)* than in wild-type worms, continuously decreased during a 1-min stimulus until they became weaker than those in the wild type after ~40 s (**Fig. 3e**).

DISCUSSION

OptIoN greatly simplifies current electrophysiological protocols by obviating the requirement for damaging electrical stimulation[6,7]. Further, photostimulation is technically far more versatile than electrical stimulation: photo-ePSCs can be induced at high frequency and under sustained stimulation. Our method thus opens up the *C. elegans* system to studies of synaptic plasticity. OptIoN also allows, to our knowledge for the first time, to trigger GABA release at the neuromuscular junctions. Therefore it will provide insight into genes that regulate the synaptic function of GABAergic neurons.

OptIoN complements presently available methods for behavioral analysis of neurotransmission in *C. elegans*. Currently postsynaptic defects are most commonly characterized at the behavioral level by measuring the resistance of worms to nicotinic acetylcholine receptor (nAChR) or $GABA_AR$ agonists. Presynaptic impairment is typically analyzed by the resistance to the ACh-esterase inhibitor aldicarb; this readout is indirectly also sensitive to defective GABA transmission. Yet these methods lack the temporal precision of OptIoN: pharmacologically induced paralysis is typically quantified after minutes to hours, whereas light-induced effects occur instantly. Moreover, the light stimulus can be turned off immediately, whereas agonists can not be removed on a reasonable time scale, which impedes repeated stimulation.

Although behavioral analyses by OptIoN can report on the existence of synaptic abnormalities, the physiological nature of synaptic defects cannot be determined solely based on behavioral assays. Presynaptic mutations that reduce ACh release caused increased light-evoked contractions, just as enhanced ACh release in the presence of phorbol esters did (**Supplementary Fig. 5**). Although this is likely due to a compensatory increase in muscle excitability in mutants with reduced ACh release, we cannot exclude other reasons (see **Supplementary Results**). In general, therefore, additional analyses of mutants that show behavioral changes are required. Furthermore, continuous photostimulation caused sustained behavioral changes, whereas steady-state photo-ePSCs were small compared to the initial peak currents. It is thus not clear how sustained behavior and ePSCs (the latter measured in dissected worms) correspond to each other; this may cause discrepancies in results obtained by the two approaches.

Another concern with the behavioral analyses might be that the effects may be sensitive to body size; this is relevant because many presynaptic mutants are smaller than wild-type worms. We compared adult and larval stage four (L4) worms, which are about half the size of adults (**Supplementary Fig. 1d,e**). Normalized GABA-evoked elongations did not differ, and there was a weak positive correlation between body size and extent of ACh-mediated contractions. Thus, if at all, defects in small mutants would only be underestimated.

Postsynaptic mutations can also be analyzed by OptIoN, as exemplified by our analysis of *unc-49* $GABA_AR$ mutants. Photostimulating endogenous transmitter release has advantages over exogenous agonist application: LED illumination provides submillisecond accuracy, and transmitter release is independent of application pipettes, is likely to occur at physiological concentrations and is restricted to synaptic contacts. Thus OptIoN may allow behavioral and physiological analysis also of mutants with dispersed postsynaptic receptors.

Although this study is focused on *C. elegans* neuromuscular junctions, the same principle may be applicable to other model systems such as *Drosophila melanogaster*. Central and peripheral synapses in rodent models may be similarly accessible to optogenetics-assisted analyses of synaptic function, not only with electrophysiological approaches but possibly also by choosing quantifiable evoked behaviors.

METHODS

Behavioral experiments. Transgenic worms were cultivated in the dark at 20 °C on nematode growth medium (NGM)[8] plates with OP50 bacteria without or with all-*trans* retinal. Plates containing all-*trans* retinal were prepared by spreading 300 µl of OP50 culture mixed with 0.25 µl of 100 mM all-*trans* retinal stock (dissolved in ethanol) onto 5.5-cm plates containing 10 ml of NGM. About 18 h before experiments, L4 larvae, grown on all-*trans* retinal plates, were placed on fresh all-*trans* retinal plates (containing 2 µg/ml phorbol-12-myristate-13-acetate (Sigma), in the case of phorbol ester experiments). Worms were illuminated

with blue light (1.6 mW/mm^2) from a 50-W mercury lamp, filtered through a GFP excitation filter (450–490 nm), on 3.5-cm diameter plates containing 750 µl of NGM, under a 10× objective in a Zeiss Axiovert40 microscope. Duration of illumination was defined by a computer-controlled shutter (Sutter Instruments). Worms were filmed with a Powershot G5 digital camera (Canon) at 320 × 240 resolution, with 4× optical zoom, and body length was determined as previously described[11]. One pixel corresponds to ~3 µm, and for an adult worm (~1 mm, or about 300 pixels), the experimental error is ~0.3% of the body length. For analyzing swimming behavior, worms were washed with M9 buffer and placed into 96-well plates containing 80 µl NGM and 80 µl of M9 buffer per well. Worms were filmed during illumination, and swimming cycles (the worm's body bends twice per cycle), full and half, were counted.

Quantitative behavioral analysis. Individual images, extracted as consecutive frames from video microscopy of behaving worms, were processed using Matlab (Mathworks) to extract the worm's body from background[21]. Cases of self-intersection were excluded from processing. Images of worms were skeletonized to a single-pixel-thick backbone and the body length recorded as the backbone length. Worm lengths were normalized by the mean length (averaged over 15 frames) before the photostimulation and followed over hundreds of consecutive movie frames (at 15 Hz). Length chronograms of multiple worms were then averaged and the profiles compared between wild type and mutants. For all analyses, significance compared to wild type after two-tailed Student's *t*-test is given as *P*-values.

Additional methods. Descriptions of plasmid construction, generation of transgenic and mutant worms, electrophysiological recordings and fluorescence microscopy are available in **Supplementary Methods** online.

Note: Supplementary information is available on the Nature Methods website.

ACKNOWLEDGMENTS

We thank M. Nonet for helpful comments on the manuscript, J. Rand (Oklahoma Medical Research Foundation) for the P*unc-17* plasmid, D. Miller III (Vanderbilt University) for the P*unc-4* plasmid, E. Jorgensen (University of Utah) and the *Caenorhabditis* Genetics Center for strains, and K. Zehl for expert technical assistance. We thank the lab of Prof. R. Tampé for hospitality and ongoing support. This work was funded by the Goethe University, Frankfurt, grants from the Deutsche Forschungsgemeinschaft to A.G. (SFB628 and GO 1011/2-1), and the Cluster of Excellence Frankfurt, Macromolecular Complexes, and grants from Canadian Institute of Health Research (MOP-79404 and MOP-74530) to M.Z.; G.J.S. was supported in part by the US National Institutes of Health (R01 EY017241, P50 MH062196) and by the Swartz Foundation.

AUTHOR CONTRIBUTIONS

J.F.L., Mar.B., Mag.B. and A.G. designed the experiments; J.F.L., Mar.B., Mag.B. and C.S. performed the experiments; G.J.S. wrote software and performed automated analysis of worm shape; J.F.L., Mar.B., Mag.B. and A.G. performed all other data analysis; and Mar.B., J.F.L., M.Z., Mag.B. and A.G. wrote the manuscript.

Published online at http://www.nature.com/naturemethods/
Reprints and permissions information is available online at http://npg.nature.com/reprintsandpermissions/

1. Wojcik, S.M. & Brose, N. Regulation of membrane fusion in synaptic excitation-secretion coupling: speed and accuracy matter. *Neuron* **55**, 11–24 (2007).
2. Richmond, J.E. Synaptic function. In *WormBook* (ed., The *C. elegans* Research Community) (doi/10.1895/wormbook.1.69.1; 2005).
3. Richmond, J.E. & Jorgensen, E.M. One GABA and two acetylcholine receptors function at the *C. elegans* neuromuscular junction. *Nat. Neurosci.* **2**, 791–797 (1999).
4. Guerrero, G. *et al.* Heterogeneity in synaptic transmission along a *Drosophila* larval motor axon. *Nat. Neurosci.* **8**, 1188–1196 (2005).
5. Miller, K.G. *et al.* A genetic selection for *Caenorhabditis elegans* synaptic transmission mutants. *Proc. Natl. Acad. Sci. USA* **93**, 12593–12598 (1996).
6. Richmond, J.E. Electrophysiological recordings from the neuromuscular junction of *C. elegans*. In *WormBook* (ed., The *C. elegans* Research Community) (doi/10.1895/wormbook.1.112.1; 2006).
7. Francis, M.M., Mellem, J.E. & Maricq, A.V. Bridging the gap between genes and behavior: recent advances in the electrophysiological analysis of neural function in *Caenorhabditis elegans*. *Trends Neurosci.* **26**, 90–99 (2003).
8. Brenner, S. The genetics of *Caenorhabditis elegans*. *Genetics* **77**, 71–94 (1974).
9. Schuske, K.R. *et al.* Endophilin is required for synaptic vesicle endocytosis by localizing synaptojanin. *Neuron* **40**, 749–762 (2003).
10. Nagel, G. *et al.* Channelrhodopsin-2, a directly light-gated cation-selective membrane channel. *Proc. Natl. Acad. Sci. USA* **100**, 13940–13945 (2003).
11. Nagel, G. *et al.* Light activation of channelrhodopsin-2 in excitable cells of *Caenorhabditis elegans* triggers rapid behavioral responses. *Curr. Biol.* **15**, 2279–2284 (2005).
12. Zhang, F. *et al.* Multimodal fast optical interrogation of neural circuitry. *Nature* **446**, 633–639 (2007).
13. Boyden, E.S., Zhang, F., Bamberg, E., Nagel, G. & Deisseroth, K. Millisecond-timescale, genetically targeted optical control of neural activity. *Nat. Neurosci.* **8**, 1263–1268 (2005).
14. Li, X. *et al.* Fast noninvasive activation and inhibition of neural and network activity by vertebrate rhodopsin and green algae channelrhodopsin. *Proc. Natl. Acad. Sci. USA* **102**, 17816–17821 (2005).
15. Zhang, Y.P. & Oertner, T.G. Optical induction of synaptic plasticity using a light-sensitive channel. *Nat. Methods* **4**, 139–141 (2007).
16. White, J.G., Southgate, E., Thomson, J.N. & Brenner, S. The structure of the nervous system of the nematode *Caenorhabditis elegans*. *Phil. Trans. R. Soc. Lond. B* **314**, 1–340 (1986).
17. McIntire, S.L., Reimer, R.J., Schuske, K., Edwards, R.H. & Jorgensen, E.M. Identification and characterization of the vesicular GABA transporter. *Nature* **389**, 870–876 (1997).
18. Alfonso, A., Grundahl, K., Duerr, J.S., Han, H.P. & Rand, J.B. The *Caenorhabditis elegans* unc-17 gene: a putative vesicular acetylcholine transporter. *Science* **261**, 617–619 (1993).
19. McIntire, S.L., Jorgensen, E., Kaplan, J. & Horvitz, H.R. The GABAergic nervous system of *Caenorhabditis elegans*. *Nature* **364**, 337–341 (1993).
20. Bamber, B.A., Beg, A.A., Twyman, R.E. & Jorgensen, E.M. The *Caenorhabditis elegans* unc-49 locus encodes multiple subunits of a heteromultimeric GABA receptor. *J. Neurosci.* **19**, 5348–5359 (1999).
21. Stephens, G.J., Johnson-Kerner, B., Bialek, W. & Ryu, W.S. Dimensionality and dynamics in the behavior of *C. elegans*. *PLoS Comput. Biol.* **4**, e1000028 (2008).
22. Liu, Q. *et al.* Presynaptic ryanodine receptors are required for normal quantal size at the *Caenorhabditis elegans* neuromuscular junction. *J. Neurosci.* **25**, 6745–6754 (2005).
23. Hammarlund, M., Palfreyman, M.T., Watanabe, S., Olsen, S. & Jorgensen, E.M. Open syntaxin docks synaptic vesicles. *PLoS Biol.* **5**, e198 (2007).
24. Richmond, J.E., Weimer, R.M. & Jorgensen, E.M. An open form of syntaxin bypasses the requirement for UNC-13 in vesicle priming. *Nature* **412**, 338–341 (2001).
25. Nonet, M.L., Saifee, O., Zhao, H., Rand, J.B. & Wei, L. Synaptic transmission deficits in *Caenorhabditis elegans* synaptobrevin mutants. *J. Neurosci.* **18**, 70–80 (1998).
26. Jorgensen, E.M. *et al.* Defective recycling of synaptic vesicles in synaptotagmin mutants of *Caenorhabditis elegans*. *Nature* **378**, 196–199 (1995).
27. Zhang, J.Z., Davletov, B.A., Sudhof, T.C. & Anderson, R.G. Synaptotagmin I is a high affinity receptor for clathrin AP-2: implications for membrane recycling. *Cell* **78**, 751–760 (1994).
28. Richmond, J.E., Davis, W.S. & Jorgensen, E.M. UNC-13 is required for synaptic vesicle fusion in *C. elegans*. *Nat. Neurosci.* **2**, 959–964 (1999).
29. Harris, T.W., Hartwieg, E., Horvitz, H.R. & Jorgensen, E.M. Mutations in synaptojanin disrupt synaptic vesicle recycling. *J. Cell Biol.* **150**, 589–600 (2000).
30. Nonet, M.L. *et al.* UNC-11, a *Caenorhabditis elegans* AP180 homologue, regulates the size and protein composition of synaptic vesicles. *Mol. Biol. Cell* **10**, 2343–2360 (1999).